Effect of post-weld heat treatment on thermal diffusivity in UNS S32304 duplex stainless steel welds

**E.G. Betini [a,*], C.S. Mucsi [a], T.S. Luz [b], M.T.D. Orlando [b],
M-N. Avettand-Fènoël [c], J.L. Rossi [a]**

[a] Nuclear and Energy Research Institute (IPEN),
Av. Lineu Prestes, 2242, 05508-000, São Paulo, Brasil
[b] Mechanical Engineering Department, Federal University of Espírito Santo,
Av. Fernando Ferrari, 514, 29075-910, Vitória, Espírito Santo, Brasil
[c] Unité Matériaux et Transformations, Université Lille, 1- Cité Scientifique,
59650 Villeneuve d'Ascq, France
* Corresponding e-mail address: evandrobetini@gmail.com

ABSTRACT

Purpose: The thermal diffusivity variation of UNS S32304 duplex stainless steel welds was studied after pulsed GTA welding autogenous process without filler addition. This property was measured in the transverse section of thin plates after welding process and post-heat treated at 750°C for 8 h followed by air-cooling.

Design/methodology/approach: The present work reports measurements of thermal diffusivity using the laser-flash method. The thermal cycles of welding were acquired during welding by means of k-type thermocouples in regions near the weld joint. The used shielding gas was pure argon and 98% argon plus 2% of nitrogen. The temperature profiles were obtained using a digital data acquisition system.

Findings: It was found an increase of thermal diffusivity after welding process and a decrease of these values after the heat treatment regarding the solidified weld pool zone, irrespective of the welding protection atmosphere. The microstructure was characterized and an increase of austenite phase in the solidified and heat-affected zones was observed for post-weld heat-treated samples.

Research limitations/implications: It suggests more investigation and new measurements about the influence of the shielding gas variation on thermal diffusivity in the heat-affected zone.

Practical implications: The nuclear industry, especially, requests alloys with high thermal stability in pipes for power generation systems and safe transportation equipment's for radioactive material. Thus, the duplex stainless steel grades have improved this stability over standard grades and potentially increase the upper service temperature reliability of the equipment.

Originality/value: After heat treatment, the welded plate with 98%Ar plus 2%N_2 as shielding gas presented a thermal diffusivity closer to the as received sample. By means of 2%-nitrogen addition in shielding gas during GTAW welding of duplex stainless steel may facilitate austenite phase reformation, and then promotes stability on the thermal diffusivity of duplex stainless steels alloys.

PROPERTIES

1. Introduction

Duplex stainless steels (DSS) have basically ferritic-austenitic microstructure that combines excellent mechanical properties and efficient weldability [1]. DSS are desirable for many applications because of their attractive combination of mechanical strength, corrosion resistance and cost. The last two decades have seen a trend towards a growing application of duplex stainless steel (DSS) [1]. The nuclear industry, especially, requests alloys with high thermal stability in pipes for power generation systems and safe transportation equipment's for radioactive material. Transport devices of Mo-99 (radioactivity above 16.2 Ci) are built to requirements specified by standard regulation according to nuclear safety commissions. During the validation tests, the stainless steel selected as external shield must be able to withstand 30 minutes in an 800°C fire [2,3]. Thus, new lean grade DSS alloys have improved this stability over standard grades and potentially increase the upper service temperature reliability of the equipment [4,5].

The heat transfer processes and the thermal cycles for a given dimension of a metal part are sensitive to variations of thermal diffusivity and thermal capacity [2]. The microstructure and mechanical properties of a metallic component are dependent upon the welding processes and further thermal treatment that the part is subjected. In order to promote the application of DSS, considerable efforts have been devoted to obtain better understanding of the influence of metallurgical factors on the weldability of such steels [4].

The weldability of DSS is satisfactory, although the heat affected zone and weld pool metal generally exhibit higher ferrite content and coarser grains than the original material [4,6]. Duplex steel with moderate nitrogen content solidifies ferritically [4]. During welding the austenite dissolves while being heated, it is followed by grain growth in the delta ferrite region, and finally restoring to the austenitic phase during cooling [6]. However, an increased amount of N is beneficial for the austenite restoring. Nitrogen, as one of the strongest austenite forming alloying elements, is an economical and efficient substitute for nickel [7]. It also contributes to high strength and corrosion resistance. The addition of N should be optimized, close to the upper limit, and losses of N during welding should be minimized [1,8]. The desired ferrite-austenite phase balance can also be achieved by a high heat input weld, which provides a slow cooling and promotes the desired phase balance [6,8]. Nowadays, several studies have been focused on post-weld heat treatment (PWHT) for DSS weld joints in order to get an optimal phase balance [9,10,11]. Zhang et al [10] investigated the effect of short-time PWHT on microstructure and corrosion resistance of UNS S31803 duplex stainless steel. After PWHT, it was observed that the volume fraction of austenite in the heat affected zone and weld metal was significantly increased. Badji et al. [11] observed the effect of PWHT in the range of 800°C-1150°C on the microstructure and on the mechanical property of welded UNS S32205 duplex stainless steel and found the PWHT temperature lower than 1100°C leads to higher microhardness due to the σ phase precipitation in the ferrite phase. Finally, Saravanan et al. [12] used pulsed Nd:YAG laser welding machine and as-weld DSS joints subjected to post weld heat treatment (PWHT) at 1050°C for 2 h to increase the amount of austenite phase. This lessens the phase imbalance and improves the corrosion properties of SDSS laser welds.

F. H. Ley et al. [13] studied the effect of the shielding gas variation on thermal properties in the GMAW welding process. It was observed an influence of the shielding gas on the thermal expansion, thermal diffusivity and thermal conductivity of the weld metal compared to the base metal (DH36 steel plate). Abas R. H. and Taieh, N. K. [14] measured the thermal diffusivity and thermal capacity (from 1473 K until ambient temperature) for different duplex steels in order to complement the thermo physical data of these alloys. Betini et al [15] also found low value for thermal diffusivity for pure argon as shielding gas using conventional GTA welding process in heat-affected region. Matteis P. et al. [16] reported a linear decrease of the thermal diffusivity occurring in low-alloy austenite steels during the cooling process. Furthermore, it was defined that the thermal diffusivity is the most influent thermophysical

property in quenching processes that can be analysed by thermo-metallurgical models.

In the present work, it was proposed a study of the thermal diffusivity of the UNS S32304 thin plates in the solidified zone (SZ), heat affected zone (HAZ) and base metal (BM) after GTAW welding without metal addition (autogenous). The effect of aging at 750°C for 8 h on the thermal diffusivity and microstructural evolution of the UNS S32304 duplex stainless steel welds were also reported.

2. Experimental

The specimens were obtained with dimensions of 72 x 72 x 1.8 mm^3. Table 1 shows typical chemical composition of UNS S32304 duplex stainless steel (mass %). The alloy

chemical composition was certified by the commercial supplier Aperam Inox América do Sul S/A. The heterogeneous microstructure of the ferrite and austenite was observed using optical microscopy. The post-weld heat treatment (PWHT) was carried out at 750°C for 8 h in a muffle furnace in air. After that, the samples were taken out and air-cooled. The specimens for microstructure investigation were ground successively from 800, 1200 and 2000 grit, and polished using diamond pastes of 6, 3 and 1 μm. The metallographic samples were etched with Behara I solution for 15 s to 20 s. To observe the dual-phase microstructure of the as polished specimens after PWHT, the samples were the electrochemically etched in a 10% oxalic acid solution for 20 s. The optical microstructures of the SZ and HAZ were observed by means of the Image J® software with optical microscope. The percentages of the phases were calculated using image analysis techniques.

Table 1.
Chemical composition (% mass and ppm) of the duplex stainless steel UNS S32304

Cr	Ni	Mo	Mn	Si	C	P	S	Ti	Cu	Co	N ppm
22.201	3.521	0.255	1.402	0.250	0.016	0.023	0.001	0.004	0.417	0.091	1030

The plates were welded at the Welding Laboratory of the Federal University of Espírito Santo (LabSolda/DEM/UFES). The GTAW (gas tungsten arc welding) with pulsed current and direct polarities were used with automatic drive systems. The samples were fixed in order to reproduce the conventional set welding process, as shown in Fig. 1. A batch of samples was welded with commercial argon protection gas and other with a mixture of Ar and 2% of N$_2$. The gas flow rate in both cases was 10 L·min^{-1}.
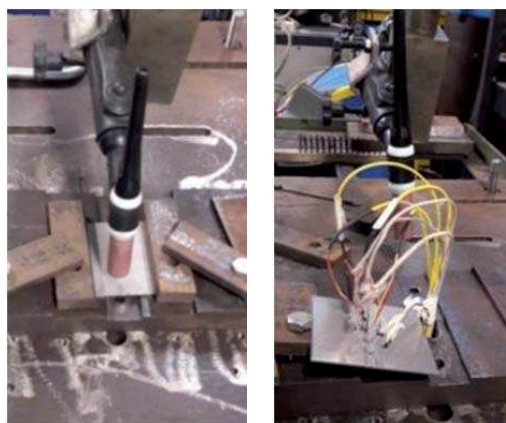

Fig. 1. Welding arrangement for the duplex stainless steel UNS S32304 thin plates

The electrical current and voltage values were measured for each welding step. The AWS Class EWTh-2 electrode was kept negative and was located at 2 mm with a 60° angle from the plate, according to direct polarity process. In the case of the pulsed current, the wave was maintained in balance with background time and pulse values equal to 0.9 s. Table 2 indicates the welding and thermal cycle parameters.

Table 2.
Welding parameters used for the pulsed GTAW process

Sample	#1A	#2AN
Shielding gas (10 L.min^{-1})	Pure Ar	Ar+2%N$_2$
Voltage	11 V	11 V
Pulse current (I$_p$)	150 A	140 A
Background current (I$_b$)	80 A	70 A
Pulse time (t$_p$)	0.9 ms	0.9 ms
Background time (t$_b$)	0.9 ms	0.9 ms
Welding speed	35 cm·min^{-1}	35 cm·min^{-1}
Arc efficiency	60%	60%
Heat input	0.20 kJmm^{-1}	0.17 kJmm^{-1}

Regarding the parameters such as voltage (U), pulsed and background current (I$_p$, I$_b$), pulsed and background time (t$_p$, t$_b$), the welding speed (v) along with 60% arc

efficiency for the pulsed GTA welding, it was possible to calculate the welding heat input (H) per mm using Eq. 1 [17]. The welding heat input shown in Table 2 was determined using the average voltage, current and welding speed.

$$H = \frac{60.U.(Ip.tp+Ib.tb)}{(tp+tb).v} \qquad (1)$$

The temperature was measured and recorded using k-type thermocouples attached to a digital data logging system. Six thermocouples were positioned and fixed to the sample plate surface using spot welding at different distances along a line perpendicular to the weld bead. Three thermocouples were attached on one side (1-3 – side A) of the plate and other three thermocouples on the other side (4-6 – side B) being given the distances from the centre of the weld nugget as shown in Fig. 1. The thermocouples distances from the joint line were: 8 mm, 13 mm and 18 mm for thermocouples 1, 2 and 3, respectively, from side A; and 10.5 mm, 13 mm and 18 mm for thermocouples 4, 5 and 6, respectively, from side B. The signals from the thermocouples were acquired with a 8-channel digital data acquisition system (DAQ) amplifier using MX board – PT1000 for room temperature automatic conditioning. The measured total error limit at 295 K ambient temperature is ± 1 K and the temperature drift (k-type) was used K/10K ratio where the uncertainty was $\leq \pm 0.5$.

The laser pulse method (LFM) is a well-established transient-state measurement technique for measuring the thermal diffusivity. Thermal diffusivity is the thermal property that defines the speed of heat propagation by conduction during changes of temperature [18]. The higher the thermal diffusivity, the faster is the heat transfer. In this method, a flash of intense light energy is evenly applied to one face of a thin thickness sample (2 mm to 3 mm). The energy pulse diffuses unidirectional to the opposite face, allowing the recording of the transient temperature rise of this face. The block diagram of the laser flash method used in the present work is shown in Fig. 2 [15]. The thermal diffusivity is calculated from Eq. 2 [18],

$$\alpha = \frac{1.37\,L^2}{\pi^2 t_{1/2}} \qquad (2)$$

where L is the sample thickness, $t_{1/2}$ is the elapsed time for the rear-surface temperature to reach half its maximum temperature rise.

The measurement apparatus precision was verified by performing two successive series of standard flash laser measurements according to ASTM 1461 [19] on thin plates of UNS S32304 as received in room temperature (see Table 3). The difference between the measured diffusivity values and the values reported in the literature is lower than 5%, which is the repeatability of the standard laser flash measurements [14,19,20].
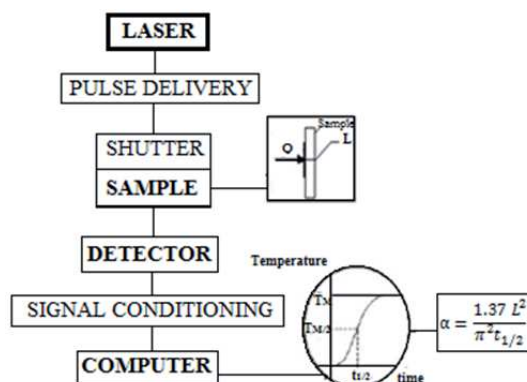

Fig. 2. Block diagram of the laser flash method used in the present work [15]

Table 3.
Experimental verification measurements of thermal diffusivity (in room temperature) via laser flash method

UNS S32304	α (10^{-6} m²/s)
Ref. 14	4.2 ± 0.2
As received	4.2 ± 0.2

A carbon dioxide (CO_2) laser with a Gaussian profile was used. The laser light wavelength is in the order of 10^{-6} m with an intensity of $10.(2)^{1/2}$ W/m² and a focus diameter of 2 mm. The temperature variations were recorded by a J-type thermocouple capable of measuring temperatures in the range of 0°C up to 480°C. An amplifying board was used to enhance the signal from the thermocouple and sent it to a computer. A model PCI AD converter 711 with 8-bit resolution processed the analogic signal. A software, developed by the High Pressure Laboratory – PRESLAB of the Federal University of Espírito Santo [21], analysed the thermal profile.

3. Results and discussion

Figure 3 defines the temperature distributions for the six thermocouples for both specimens. First, for Fig. 3 (a) the thermocouples 1 (8 mm) and 4 (10.5 mm) were placed closer to the solidified zone where the temperatures were closer to 360°C and 350°C, respectively. The thermocouples 2 and 5 with symmetrical distances from the weld line (13

mm) presented similar values of peak of temperature. This result was interesting for the validation and credibility of the experimental arrangement.
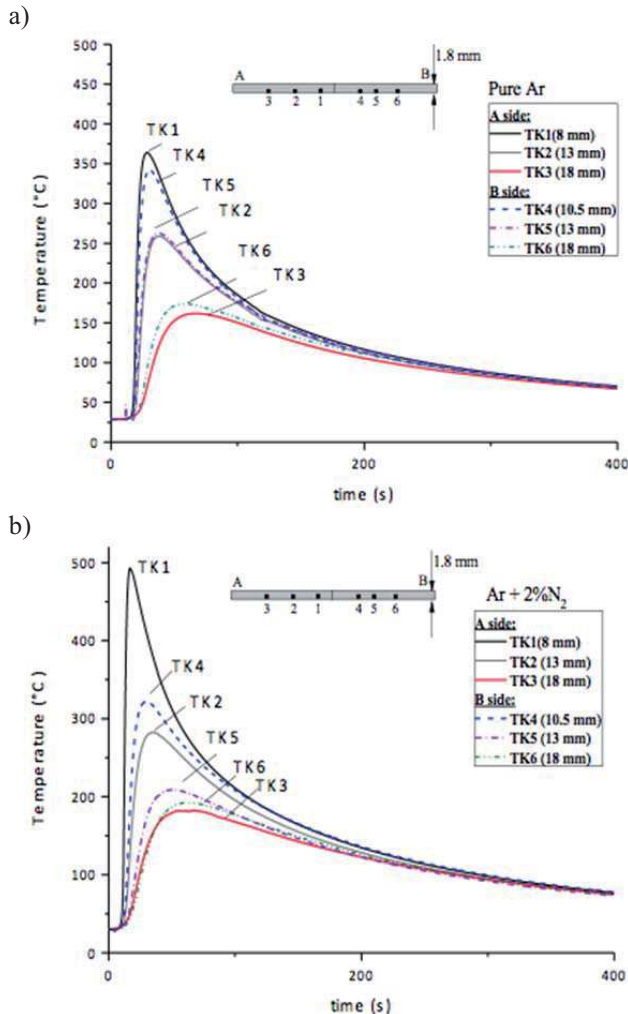
a)

b)

Fig. 3. Distribution of temperature for samples during welding with (a) pure argon and (b) Ar + 2% N_2 as shielding gas

In the temperature distribution profile for sample Ar+2%N_2 shown in Fig. 3 (b), a temperature peak near 500°C is observed for thermocouple 1 (8 mm) that is 140°C higher that reached with pure argon sample considering the same region. It has occurred due to the influence of the shielding gas used for sample Ar+2%N_2. According to Muthupandi et al. [22] and Lin et al. [23], the Ar-N_2 mixture has a higher ionization potential, increasing the welding energy and the peak temperature. The overheating in the weld joint causes changes on the cooling rates and consequently effects on the microstructural evolution.

Figure 4 presents the optical microstructure consisted of austenite and ferrite of the as received material. Ferrite phase is shown as dark contrast, while the light region is austenite phase (Fig.4. (a)). In the continuous ferrite matrix is embedded island-like austenite phase without apparent secondary phase precipitation. Both grains are elongated along the rolling direction. Fig. 4(b) shows the quantitative evaluation of the content of both ferrite and austenite phases. Based on microstructural investigations and by using image analyzer software the amounts of phases in different zones of the joints were performed. Five optical micrographs – OM images were collected for each zone (solidified zone, HAZ and BM) at 200x magnification and then were processed. The surface fractions of each phase were calculated according to ASTM E1245 standard.
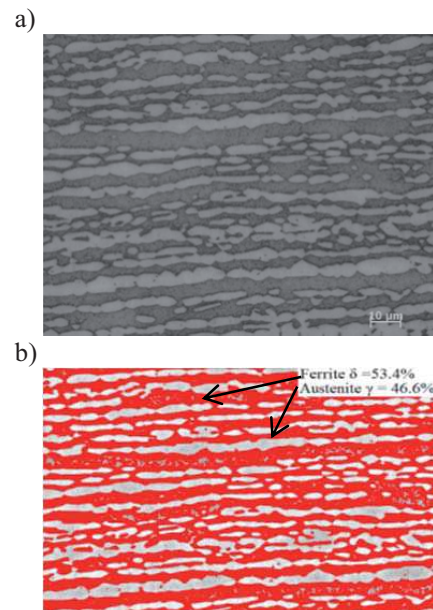
a)

b)

Fig. 4. Optical micrography (a) an exemple of phase percentage determination (b) for base metal of DSS (UNS S32304)

Figure 5 shows the effect of shielding gas composition and PWHT on the optical microstructures in HAZ and SZ of the DSS GTA welding joint. The evolution of the heat-affected zone microstructure strongly depends on the microstructure of the base metal, the peak temperature, the holding time and the cooling rates [24,25]. DSS have primary δ and γ_1 and secondary austenite γ_2, σ, χ, carbides, nitride, etc., phases [26]. In DSS weld zones, austenite phase is generally formed from ferrite in three different modes: allotriomorphic austenite at the ferrite grain boundaries (GBA), intergranular austenite (IGA) and

Widmanstätten austenite side-plates (WA) inside the grains [10,11]. As observed in Fig. 5, the microstructure of HAZ for as-welded samples with pure Ar and Ar-N$_2$ atmosphere mixture as shielding gas consists of large ferrite grains with intergranular austenite, grain boundaries austenite and Widmanstätten austenite. The HAZ exhibited low austenite because of the rapid thermal cycle [27]. It also was observed inside the ferrite matrix small secondary austenite distributed. The solidified zone (SZ) shows elongated and columnar austenite grains mainly for welding in 98%Ar+2%N$_2$ atmosphere. After PWHT, the grain boundary allotriomorphic austenite and Widmänstatten austenite increase significantly for welds with Ar-N$_2$ mixture as shielding gas. This observed microstructure is in agreement with the results of Zhang et al. [10]. In this work it was used the equilibrium phase diagram by Thermo-Calc software to calculate the total phase content of PWHT for DSS UNS S31803. It was also observed an increase of austenite content in the HAZ and solidified zone mainly after PWHT temperature from 650°C.
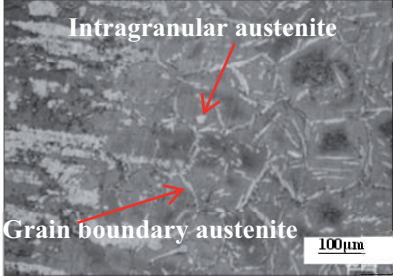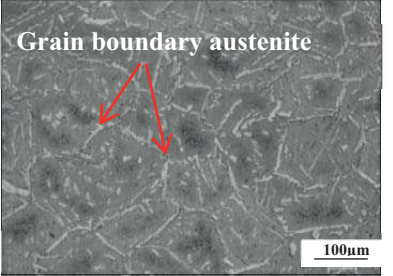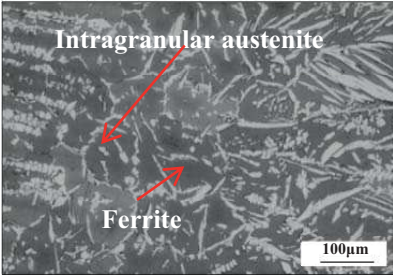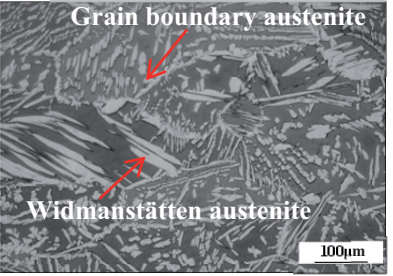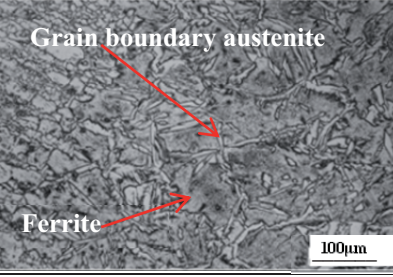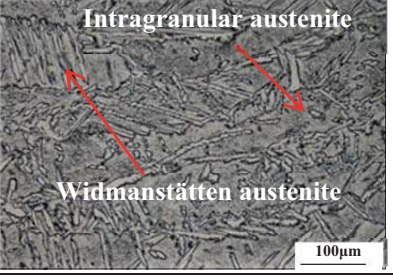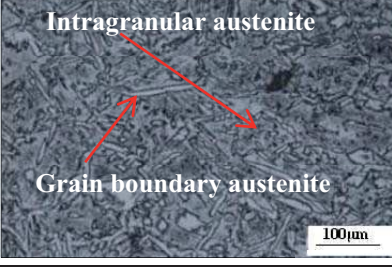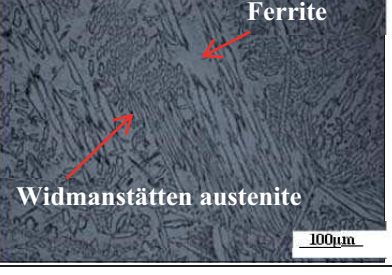

Fig. 5. Effects of pulsed GTA welding and PWHT on the optical microstructures of HAZ and solidified zone of the DSS welding joint types

Figure 6 shows the evolution of shielding gas composition on the volume fraction of austenite with PWHT in solidified zone, HAZ and BM. The percentages of austenite are significantly affected for additional nitrogen in shielding gas and it leads to changes on total austenite after heat treatment at 750°C during 8 hours. With regards the N_2-supplemented in shielding gas it was related increase of austenite content (as welded in solidified zone: 22%→37% and HAZ: 23%→25.3%), which is in agreement with the results of and Zhang et al and Taiei et al [27, 28]. After PWHT, the content of austenite phase in solidified zone and HAZ also increase around to 47 and 53% for pure Ar sample and between 55 and 57% for Ar+2%N_2, respectively. The addition of nitrogen in shielding gas significantly increased the austenite amount of DSS GTAW welds [27]. Zhang et al [27] reported that N_2-supplemented shielding gas mainly promotes the primary austenite formation, suppressed the Cr_2N precipitation in weld root. According to Westin et al [29], nitrogen can increase of transformation temperature of ferrite to austenite. Consequently, the higher nitrogen contents makes the alloys less sensible to rapid cooling rates due to more efficient austenite reformation and delays ferritization [29]. As seen, the microstructural changes in DSS that occur during welding and PWHT can lead to variation of phase balance in SZ and HAZ. Matteis et al [16] reported that the thermal diffusivity of the undercooled austenite is significantly lower than that of the ferritic constituents (i.e. pearlite, bainite or martensite) of the austenitic stainless steels.
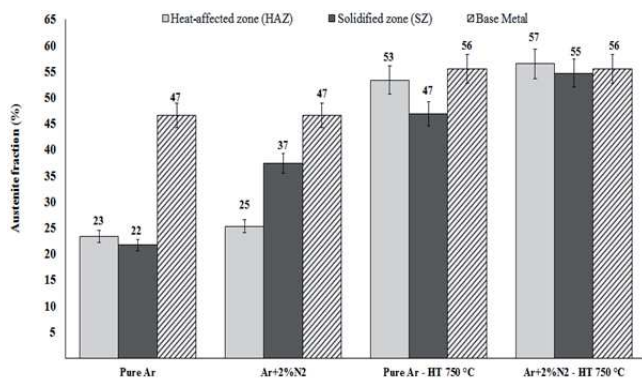

Fig. 6. Diagram for austenite content in the solidified zone, HAZ and base metal

Thus, the increase of austenitics phases (secondary, allotriomorphic, Widmanstätten and intergranular austenite) may suggest directly effects on the thermal diffusivity in DSS weldments.
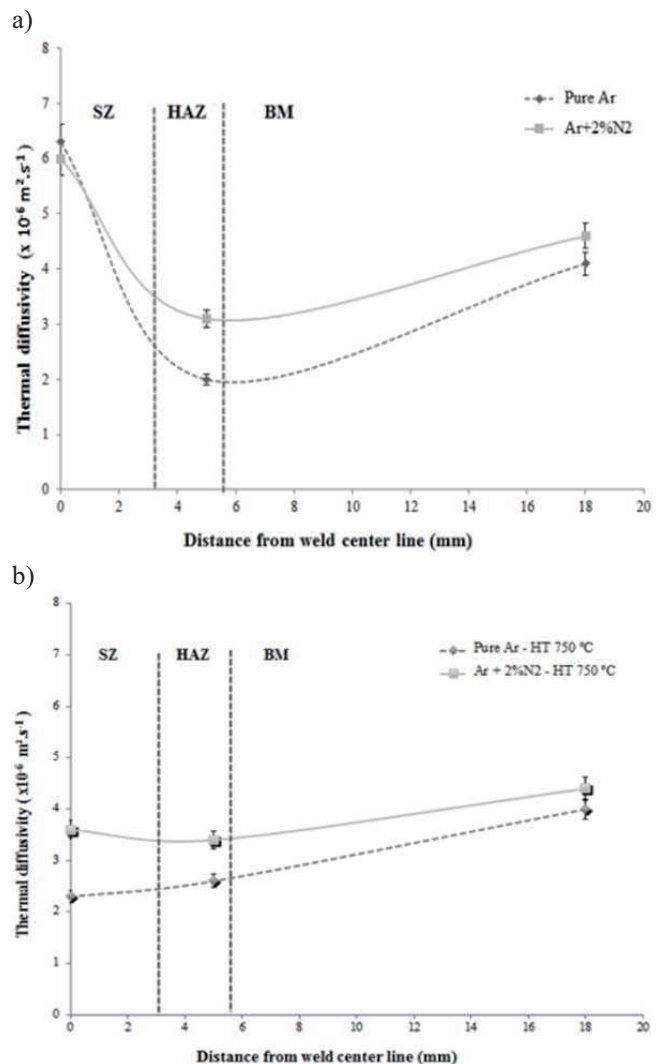
a)

b)

Fig. 7. Thermal diffusivity after pulsed GTA welding process for each region from weld line. Before heat treatment (a) and followed after heat treatment at 750°C followed by air-cooling (b)

Through thermal diffusivity measurements (Fig. 7 (a)), it is possible to observe a wide variation in the thermal diffusivity of the welded samples, mainly at the regions with higher incidence of heat during welding. It was noticed the highest value of thermal diffusivity at the molten region and a sharp decrease in this property regarding the heat affected zone (5 mm from the molten zone). In the heat-affected zone the thermal diffusivity was more affected when the welding occurred under pure argon atmosphere. The lowest value of thermal diffusivity (2.0 x 10^{-6} m²·s^{-1}) was obtained in this region. It was observed, by Betini et al [15] low values for thermal diffusivity with

pure argon shielding gas using conventional GTA welding process in molten zone and HAZ. For Ar+2%N$_2$, the change is slightly lower (3.1 x 10^{-6} m²·s^{-1} from the weld bead at 5 mm): the temperature during welding also was greater than that one of pure argon.

Figure 7 (b) shows that the PWHT procedure promoted a decrease in the thermal diffusivity in the solidified zone for both sample. It is also noted that the thermal diffusivity was less reduced for sample welded with Ar-N$_2$ mixture as shielding gas and the values remained close to the base metal. A reduction of ferrite amount was also observed for these samples after the PWHT in the same regions. Consequently, the growth observed in austenitic phase suggests further investigation about their effects on heat propagation in SZ of DSS welds.
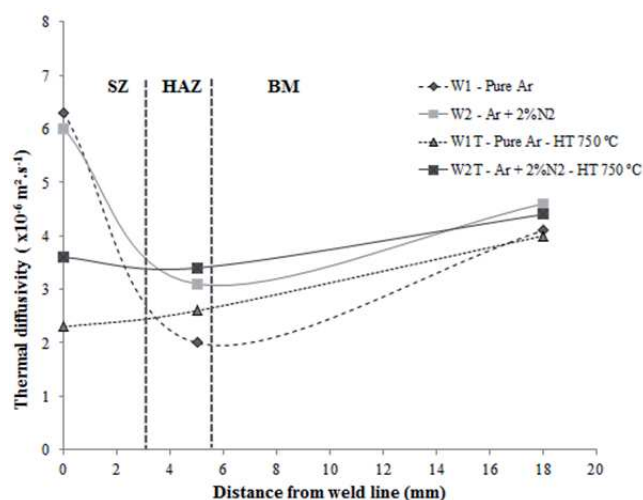

Fig. 8. Thermal diffusivity after pulsed GTA welding process for each region from the weld line according to pre-and post-heat treatment for UNS S32304 DSS welds

Figure 8 presents all measurements of thermal diffusivity. The sample welded with pure Ar as shielding gas exhibit significantly variation of thermal diffusivity values (65% less than that of before heat treatment). For Ar+2%N$_2$ sample, this variation was more slightly (36% less after PWHT). As discussed above, the nitrogen addition in shielding gas promote an increase of austenite phase and intragranular austenite generally nucleates at the inclusions and dislocations or other small precipitates such as Cr$_2$N in weld joint of GTAW weldments [22-24,27,29]. Thermal wave propagation in weld joints is influenced by microstructure characteristics, phase's amount, grain size and grain boundary, and impurities and imperfections because of welding method (heat input, shielding gas, filler metal, geometry and etc.). These parameters may

contribute to the energy dispersion of the carriers like phonons and electrons inside the material. This energy dispersion results in a decrease in the heat flow through the material [30]. Moreover, the results suggest that the nitrogen can influence to maintain the thermal diffusivity values in weld joints of DSS after heat treatment. The region away from the weld line remained close values if compared to as received samples. The thermal diffusivity measurements' error bars were between 2-5% due to the convection effects [19].

4. Conclusion

The thermal diffusivity in solidified zone, HAZ and BM of as-welded and post-welded heat treatment thin plates were investigated. The value of 4.2 x 10^{-6} m²·s^{-1} for the thermal diffusivity of UNS S32304 alloy at room temperature determined using LFM is in agreement with literature values. The heat propagation behaviour of UNS S32304 duplex stainless steel welded by pulsed GTAW may be associated with unbalanced ferrite/austenite phase ratio and precipitation process due to the high peak of temperature and fast cooling rate during welding process. An increase around 32% of thermal diffusivity in solidified zone was observed for both welded plates, while austenite phase is significantly decreased in this region. In the heat-affected zone, the thermal diffusivity was decreased mainly when the welding occurred under pure argon atmosphere.

After PWHT, the thermal diffusivity values are reduced in the solidified zone for both samples. In case of pure Ar as shielding gas, the decrease of thermal diffusivity is 65% less than after heat treatment. The volume fraction of austenite in both solidified zone and HAZ rises after PWHT at 750°C for 8 h followed by air-cooling. It also was observed a growth of austenitic phases from ferrite grain boundaries in solidified zone for plate welded with 98%Ar+2%N$_2$ as shielding gas. Furthermore, for this sample the thermal diffusivity in the solidified zone and HAZ was remained more close to the base metal values. By means of 2%-nitrogen addition in shielding gas during GTAW welding of duplex stainless steel may facilitate austenite phase reformation, and then promotes thermal stability for duplex stainless steels alloys.

References

[1] V.A. Hosseini, S. Wessman, K. Hurtig, L. Karlsson, Nitrogen loss and effects on microstructure in multipass TIG welding of a super duplex stainless steel, Materials & Design 98 (2016) 88-97.

[2] J.D. Tucker, M.K. Miller, G.A. Young, Assessment of thermal embrittlement in duplex stainless steels 2003 and 2205 for nuclear power applications, Acta Materialia 87 (2015) 15-24.

[3] E.G. Betini, F.C. Ceoni, C.S. Mucsi, R. Politano, M.T.D. Orlando, J.L. Rossi, Study of the temperature distribution on welded thin plates of duplex steel to be used for the external clad of a cask for transportation of radiopharmaceuticals products, Proceedings of the International Nuclear Atlantic Conference – INAC, 2015, São Paulo-SP, Brazil, 1-6.

[4] G.E. Totten, C.E. Bates, N.A. Clinton, Handbook of Quenchants and Quenching Technology, ASM International, 1993.

[5] J.-O. Nilsson, Super duplex stainless steels, Materials Science and Technology 8/8 (1992) 685-700.

[6] S. Henrik, R. Sandström, Austenite reformation in the heat-affected zone of duplex stainless steel 2205, Materials Science and Engineering A 418/1 (2006) 250-256.

[7] J. Li, Z. Ma, X. Xiao, J. Zhao, L. Jiang, On the behavior of nitrogen in a low-Ni high-Mn super duplex stainless steel, Materials & Design. 32 (2011) 2199-2205.

[8] S. Hertzman, B. Brolund, P.J. Ferreira, An experimental and theoretical study of heat-affected zone austenite reformation in three duplex stainless steels, Metallurgical and Materials Transactions A 28/2 (1997) 277-285.

[9] V. Muthupandi, P.B. Srinivasan, S.K. Seshadri, S. Sundaresan, Effect of weld metal chemistry and heat input on the structure and properties of duplex stainless steel welds, Materials Science and Engineering A 358/1 (2003) 9-16.

[10] Z. Zhang, Z. Wang, Y. Jiang, H. Tan, D. Han, Y. Guo, J. Li, Effect of post-weld heat treatment on microstructure evolution and pitting corrosion behavior of UNS S31803 duplex stainless steel welds, Corrosion Science 62 (2012) 42-50.

[11] R. Badji, B. Belkessa, H. Maza, M. Bouabdallah, B. Bacroix, C. Kahloun, Effect of post weld heat treatment on microstructure and mechanical properties of welded 2205 duplex stainless steel, Materials Science Forum 467 (2004) 217-222.

[12] S. Saravanan, K. Raghukandan, N. Sivagurumanikandan, Pulsed Nd: YAG laser welding and subsequent post-weld heat treatment on super duplex stainless steel, Journal of Manufacturing Processes 25 (2017) 284-289.

[13] F.H. Ley, S. Campbell, A. Galloway, N. McPherson, Effect of shielding gas parameters on weld metal thermal properties in gas metal arc welding, International Journal of Advanced Manufacturing Technology 80/5 (2015) 1213-1221.

[14] R.H.A. Abas, N.K. Taieh, Experimental study of the thermal diffusivity and heat capacity concerning some duplex stainless steel, Khwarizmi Engineering Journal 11/2 (2015) 51-61.

[15] E.G. Betini, F.C. Cione, C.S. Mucsi, M.A. Colosio, J.L. Rossi, M.T.D.A. Orlando, Experimental study of the temperature distribution in welded thin plates of duplex stainless steel for automotive exhaust systems, SAE Technical Paper (2016) 2016-01-0503.

[16] P. Matteis, E. Campagnoli, D. Firrao, G. Ruscica, Thermal diffusivity measurements of metastable austenite during continuous cooling, International Journal of Thermal Sciences 47/6 (2008) 695-708.

[17] K.H. Tseng, C.P. Chou, The effect of pulsed GTA welding on the residual stress of a stainless steel weldment, Journal of Materials Processing Techno-logy 123/3 (2002) 346-353.

[18] W.J. Parker, R.J. Jenkins, C.P. Butler, G.L. Abbott, Flash method of determining thermal diffusivity, heat capacity, and thermal conductivity, Journal. Applied of Physics 32/9 (1961) 1679-1684.

[19] Standard ASTM E1461-01, Standard Test Method for Thermal Diffusivity by the Flash Method, 2001.

[20] J.R. Davies (Ed.), ASM Specialty Handbook: Stainless Steels, ASM International, USA, 1994, 291-301.

[21] E.G. Betini, Determination of Some Thermal Properties of Advanced Ceramics Doped with Rare Earth ion Ce^{4+}, Master Dissertation, Federal University of Espírito Santo-Vitória, Brazil, 2013 (in Portuguese).

[22] V. Muthupandi, P.B. Srinivasan, S.K. Seshadri, S. Sundaresan, Effect of nitrogen addition on formation of secondary austenite in duplex stainless steel weld metals and resultant properties, Science and Techno-logy of Welding and Joining 9/1 (2004) 47-52.

[23] Y.C. Lin, P.Y. Chen, Effect of nitrogen content and retained ferrite on the residual stress in austenitic

stainless steel weldments, Materials Science and Engineering A 307/1 (2001) 165-171.

[24] C.S.C. Machado, M.X. Milagre, M.T.D. Orlando, J.L. Rossi, Effect of protection gas in the residual stress profile of UNS S32304 stainless steel welded with TIG, Blucher Physics Proceedings – V Encontro Científico de Física Aplicada, 1(2), 2014, 1-4 (in Portuguese).

[25] J. Lancaster, Metallurgy of Welding, 6th Edition, Wood Head Publishing, Cambridge, 1999, 464.

[26] E. Johnson, Y.J. Kim, L.S. Chumbley, B. Gleeson, Initial phase transformation diagram determination for the CD3MN cast duplex stainless steel, Scripta Materialia 50/10 (2004) 1351-1354.

[27] Z. Zhang, H. Jing, L. Xu, Y. Han, L. Zhao, C. Zhou, Effects of nitrogen in shielding gas on microstructure evolution and localized corrosion behavior of duplex stainless steel welding joint, Applied Surface Science 404 (2017) 110-128.

[28] A. Tahaei, A.F.M. Perez, M. Merlin, F.A.R. Valdes, G.L. Garagnani, Effect of the addition of nickel powder and post weld heat treatment on the metallurgical and mechanical properties of the welded UNS S32304 duplex stainless steel, Soldagem & Inspeção 21/2 (2016) 197-208.

[29] E.M. Westin, Microstructure and Properties of Welds in the Lean Duplex Stainless Steel LDX 2101, PhD Thesis, Royal Institute of Technology, Sweden, 2010.

[30] Y. Terada, K. Ohkubo, T. Mohri, T. Suzuki, Thermal conductivity of intermetallic compounds with metallic bonding, Materials Transactions 43/12 (2002) 3167-3176.